



## Cu-Zn and Cu-Ni Bimetallic Particles Fabricated Using Ascorbic Acid and Its Role in Photodegradation of Methyl Orange

HENAM SYLVIA DEVI and THIYAM DAVID SINGH\*

Department of Chemistry, National Institute of Technology Manipur, Imphal-795 001, India

\*Corresponding author: E-mail: davidthiyam@gmail.com

Received: 3 March 2016;

Accepted: 21 May 2016;

Published online: 30 June 2016;

AJC-17977

Chemical reduction of metal salts using ascorbic acid (vitamin C) is a new and green approach in which ascorbic acid serve dual role of reducing and capping agent. Copper, zinc and nickel salts were reduced by ascorbic acid to give bimetallic nanoparticles. SEM images highlight the aggregation of nanoparticles, which is due to the high surface energy of the particles in nano range. Bimetallic particles fabricated are in the weight ratio of 4:1. Subsequent shift of surface plasma resonance band and XRD peaks indicate that the particles are not just a physical mixture of mono metallic particles. UV-visible spectra and XRD result rule out the alloy nature of the particles. Average size of the particles were calculated using XRD data and are in nano scaled. Size of the Cu, Cu-Zn and Cu-Ni particles as calculated by using Scherrer's equation are 43.47, 38.4 and 43.5 nm, respectively. In this work photo degradation of methyl orange has been studied to demonstrate the catalytic properties of mono and bimetallic particles. Bimetallic particles have superior catalytic application as compared to monometallic particles. These alloying of metals might have result in change of certain electronic configuration, which significantly increase the catalytic application of bimetallic nanoparticles.

**Keywords:** Bimetallic, Ascorbic acid, Catalytic properties, Methyl orange.

### INTRODUCTION

Bimetallic nanoparticles are a class of nanoparticles (NPs) consisting of two different metals that show a combination of properties that are associated with the two constituent metals. There are three types of bimetallic nanoparticles core-shell, heterogeneous and alloy nanoparticles depending on the mixing pattern of metal nanoparticles. Among of these nanoparticles, alloy nanoparticles show significant applications in catalytic field. Bimetallic alloy nanoparticles have higher catalytic efficacy than their monometallic counter parts due to strong synergy between metals [1,2].

Researchers have proposed and demonstrated various methods for the synthesis of bimetallic nanoparticles like co-reduction method, successive reduction method, reduction of double complexes, electrolysis of bulk of metal, radiation induced synthesis, sonochemical synthesis *etc.* [3,4]. In this work, we proposed a simple benign approach for the synthesis of nanoparticles using ascorbic acid as reducing agent and capping agent. Ascorbic acid is commonly known as vitamin C, it is one of the most potent reducing agents for biological systems [5]. Ascorbic acid is known for its antioxidant properties, which scavenge free radicals and reactive oxygen molecules. Because of this property it has been used as

antioxidant agent to avoid the oxidation of metal particles during synthesis process [6]. As such it serves dual role of reducing and capping agent in synthesis of metal nanoparticles [7].

### EXPERIMENTAL

Cupric acetate  $[(\text{CH}_3\text{COO})_2\text{Cu}\cdot\text{H}_2\text{O}]$ , zinc acetate  $[\text{Zn}(\text{O}_2\text{CH}_3)_2(\text{H}_2\text{O})_2]$ , nickel nitrate hexahydrate  $[\text{Ni}(\text{NO}_3)_2\cdot 6\text{H}_2\text{O}]$  and methyl orange were obtained from Merck Pvt. Ltd. L-ascorbic acid was purchased from Himedia company. Chemicals were used without further purification for the synthesis processes and all the solutions were synthesized using double distilled water.

#### General procedure

**Preparation of ascorbic acid solution:** 0.34 M of ascorbic acid solution was prepared by dissolving 1 g of it in 20 mL of double distilled water by stirring for 10 min. Solutions prepared were filtered and used for the synthesis process.

**Preparation of nanoparticles:** For the preparation of monometallic nanoparticles, 0.25 g of metal salts was dissolved in 20 mL of ascorbic acid and stirred for 1 h at room temperature. Bimetallic nanoparticle was prepared by weight out the Cu and Zn/Ni in the 4:1 weight ratio and dissolved in 20 mL

ascorbic acid solution. As above, the mixture was stirred for 1 h and leaves it undisturbed for 24 h. Later particles were centrifuged and washed with ethanol twice. Particles were dispersed in double distilled water and used for the study of catalytic applications.

**Study for the degradation of methyl orange:** To 20  $\mu\text{L}$  of  $10^{-3}$  M methyl orange, 50  $\mu\text{L}$  of nanoparticles was added in a 3 mL capacity cuvette and volume of the reaction mixture was made up to 2 mL by adding double distilled water and monitored under UV-visible spectroscopy by scanning in range of 200-800 nm.

**UV-visible spectroscopy:** Perkin Elmer Lambda 35 UV-visible spectrophotometer fitted with a constant temperature cell holder was used for taking all the UV-visible spectra. The absorption spectra of the prepared particles were recorded by taking the aqueous dispersion of the nanoparticles.

**X-ray diffraction:** For taking X-ray, only the dried samples were used and X-ray diffraction of samples was taken in a Phillip XRD instrument.

**Scanning electron microscopy (SEM) and energy dispersive X-ray analysis (EDAX):** Dried sample was employed for taking SEM images and EDAX. SEI quanta 250 model of SEM instrument was used for recording SEM image and EDAX data.

**Infrared spectroscopy:** IR spectra were recorded on Perkin Elmer Spectrum 2 IR spectrophotometer at room temperature. Dried sample was used to record the IR spectra.

## RESULTS AND DISCUSSION

Optical properties of monometallic and bimetallic nanoparticles were studied using UV-visible spectroscopy. UV-visible spectra of mono and bimetallic nanoparticles are given in Fig. 1. Copper nanoparticles show surface plasma resonance band at around 269.8 nm and this band is not observed in the UV-visible spectra of bimetallic nanoparticles. This sudden disappearance of the absorbance spectra in bimetallic system confirmed that the bimetallic nanoparticles are not just a physical mixture of metals but an alloy nanoparticles [8-10]. XRD pattern confirmed the crystalline nature of the so-synthesized particles. Comparative study of the XRD pattern of mono and bimetallic nanoparticles is given in Fig. 2. Diffraction pattern of bimetallic systems are slightly shifted as compared to diffraction peaks of monometallic nanoparticles and this further give the confirmation of the formation of bimetallic alloy nanoparticles [11]. Size of the Cu, Cu-Zn and Cu-Ni particles as calculated by using Scherrer's equation (a) are 43.47, 38.4 and 43.5 nm, respectively [12].

$$t = 0.9\lambda/B \cos \theta_B \quad (a)$$

where  $d$  is the mean size of the ordered crystalline,  $\lambda$  is the wavelength of the X-ray,  $B$  is the full width at half maximum in radian and  $\theta_B$  is the half of Bragg angle. SEM images highlight the aggregation of nanoparticles to give micro scaled structure particles, which may be due to the high surface energy of the nanoparticles. SEM images and EDAX of mono and bimetallic nanoparticles is given in Fig. 3. EDAX confirmed the presence of Cu, Zn and Ni metals in their respective bimetallic system in mass ratio of 4:1. Carbon and oxygen are also present in the sample, it is believed that these element

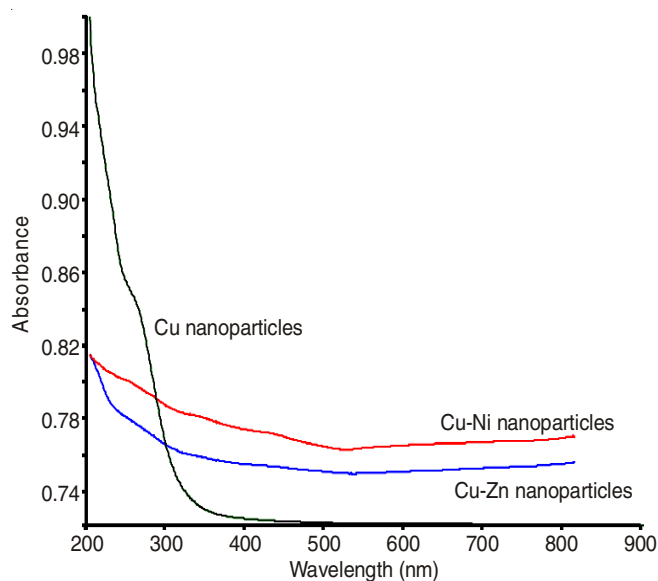


Fig. 1. UV-visible spectra of mono and bimetallic nanoparticles

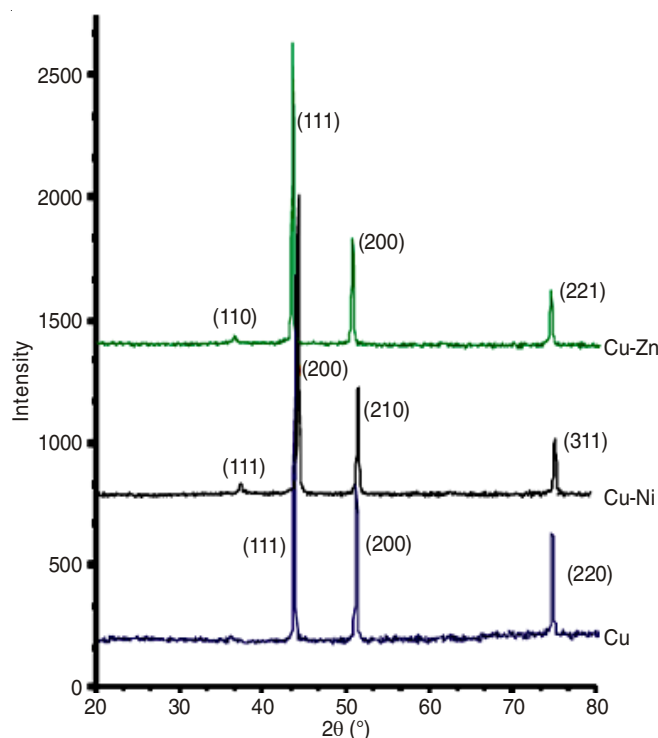


Fig. 2. XRD pattern of mono and bimetallic nanoparticles

comes from the reducing agent-ascorbic acid as it strongly bind to the nanoparticles.

IR spectra of ascorbic acid and metal nanoparticles were given in Fig. 4. From the finding obtained from IR it can be concluded that OH groups of ascorbic acid are used in the reduction of metal salt to give metal nanoparticles. Possible mechanism for the fabrication of nanoparticles is stated in **Scheme-I**. Synthesis process accompany the donation of electrons by ascorbic acid to reduces metal salt by giving semi-dehydroascorbate radical and dehydroascorbic acid [13].

Catalytic property of these nanoparticles was studied using methyl orange as role model dye for photo catalytic degradation. Methyl orange shows prominent absorbance peak at

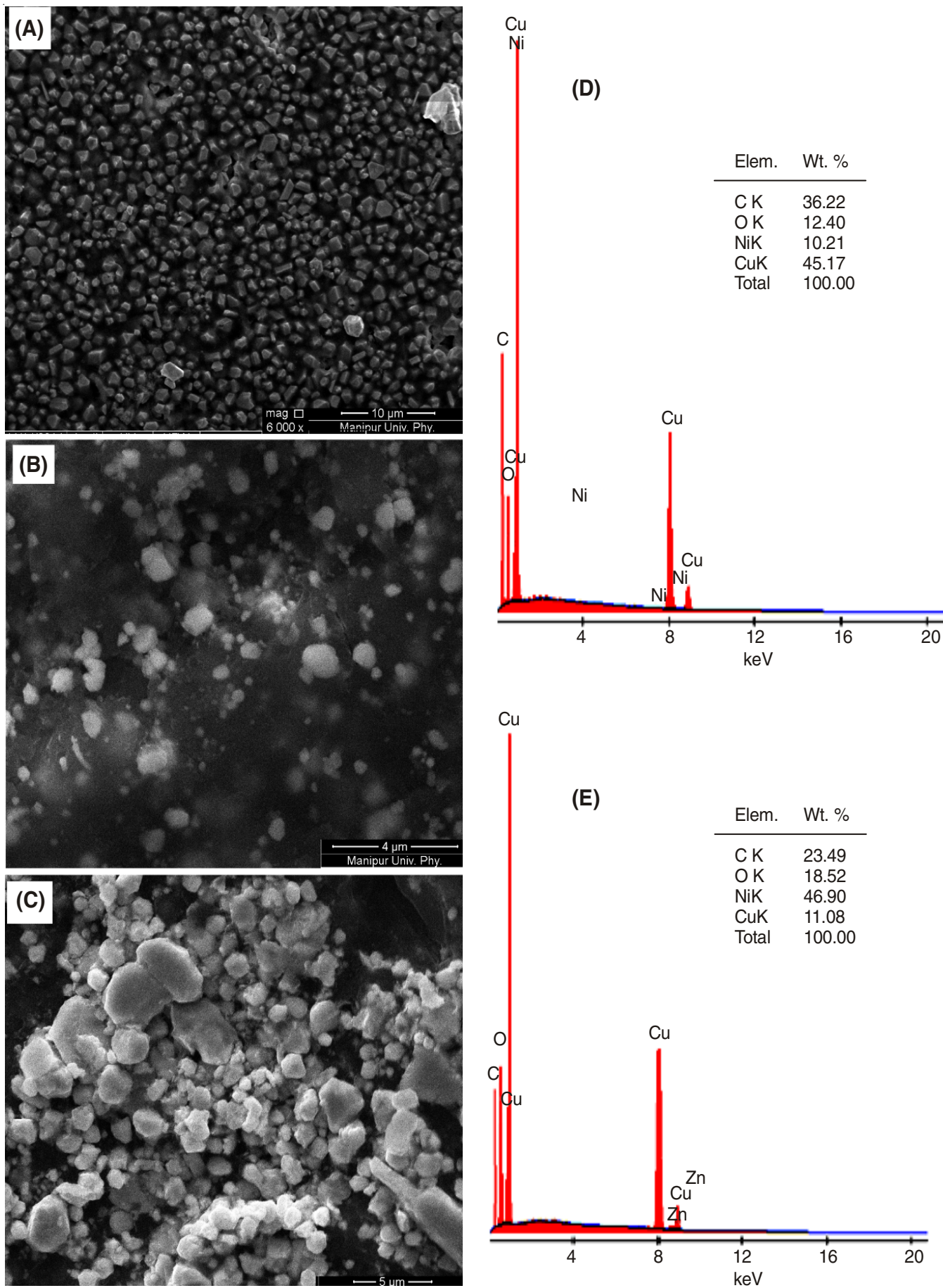
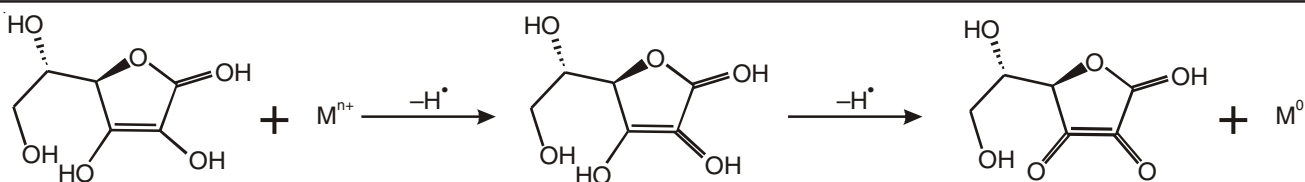


Fig. 3. SEM images of (A) Cu, (B) Cu-Zn (C) Cu-Ni, (D) EDAX of Cu-Ni and (E) EDAX of Cu-Zn nanoparticles



**Scheme-I:** Possible mechanism for the synthesis of metal nanoparticles using ascorbic acid

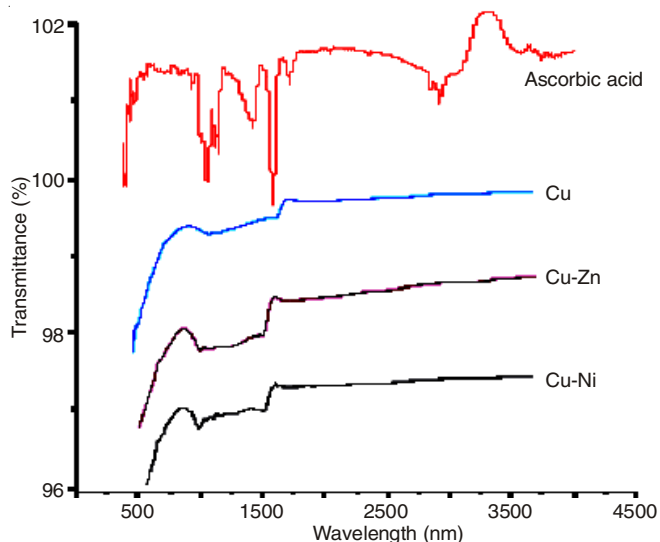


Fig. 4. IR spectra of ascorbic acid and metal nanoparticles

462.6 nm, surfacing of this peak with the addition of nanoparticles under irradiation of UV-visible light indicates the degradation of methyl orange. Fig. 5 shows that degradation of methyl orange in absence and presence of mono and bimetallic nanoparticles in 60 min. The uncatalyzed degradation of methyl orange under irradiation of UV-light is almost negligible. Degradation of methyl orange by monometallic nanoparticles is very slow as compared with the bimetallic nanoparticles, this photocatalytic degradation followed first order kinetics as predicted by plotting  $\ln A$  vs. time. Plot of  $\ln A$  vs. time (Fig. 6) give negative slope indicating that the degradation kinetics follow first order and rate constant calculated are in order  $k_{\text{Cu-Zn}} > k_{\text{Cu-Ni}} > k_{\text{Cu}}$  (Table-1). In 60 min, monometallic copper nanoparticles able to reduced 69.5 % of methyl orange while bimetallic nanoparticles Cu-Zn and Cu-Ni reduces 80.7 % and 80.4 % of methyl orange, respectively. The difference in catalytic performance between bimetallic nanoparticles and monometallic nanoparticles may be due to the electronic or

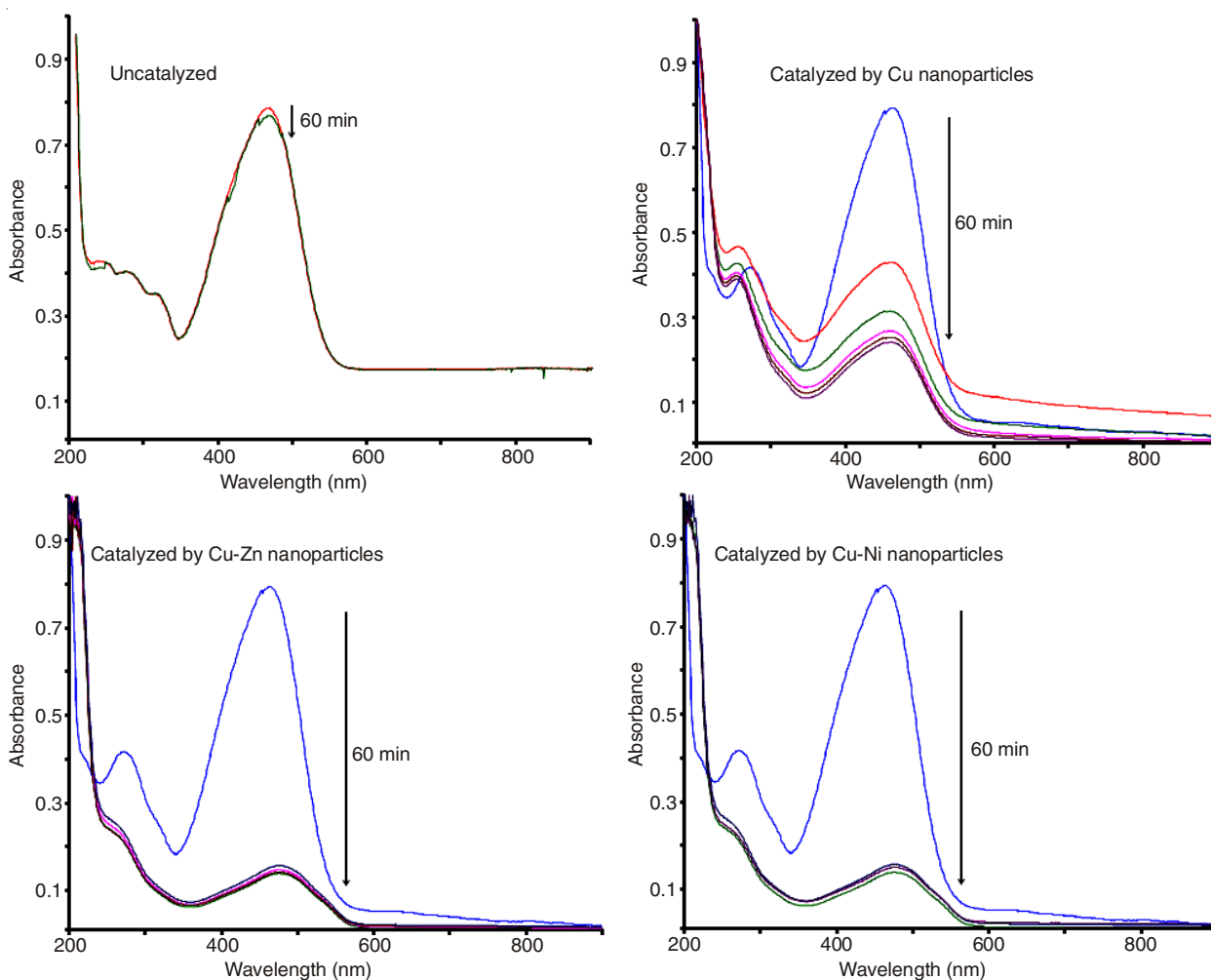


Fig. 5. UV-visible spectra of photocatalytic degradation of methyl orange using mono and bimetallic nanoparticles

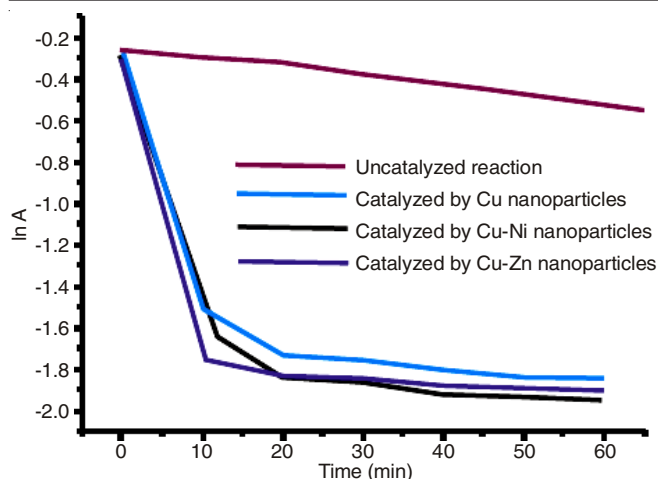


Fig. 6. Plot of  $\ln A$  vs. time for the photocatalytic degradation of methyl orange

Metal nanoparticles	Rate constant ( $\text{min}^{-1}$ )
Uncatalyzed	$1.10 \times 10^{-4}$
Cu	$1.02 \times 10^{-2}$
Cu-Ni	$1.97 \times 10^{-2}$
Cu-Zn	$2.01 \times 10^{-2}$

geometric effect result out of alloying metals [14,15]. The main reason behind this superior catalytic property of bimetallic nanoparticles is the bi-functional effect. Bi-functional effect is an effect arises between two or more entities that produce an effect greater than the sum of their individual effects. Addition of second metal significantly changes the electronic and geometric structures of nanoparticles which in turn enhance the catalytic activity [16,17]. Atoms of the two metals are active part of a catalytic site, which results in the unique role of bimetallic nanoparticles in adsorption for different reactants or different intermediates [18].

To understand the nature of interaction between methyl orange and metallic nanoparticles, the degradation reaction mixture was studied using IR spectroscopy (Fig. 7). IR spectra of methyl orange composed of asymmetric and symmetric stretching of C-H bond at  $2852 \text{ cm}^{-1}$  and  $2917 \text{ cm}^{-1}$ , respectively, band at  $2206$  and  $1994 \text{ cm}^{-1}$  are attributed to C-H bending of aromatic compound, C=C ring stretching at  $1559$  and  $1603 \text{ cm}^{-1}$ , asymmetric and symmetric stretching of S=O at  $1368$  and  $1178 \text{ cm}^{-1}$ . Bands in between  $1000$ - $800 \text{ cm}^{-1}$  is attributed to S-O stretching [19]. After treatment of methyl orange with metallic nanoparticles for 60 min, IR spectra were recorded and significant changes in the spectra were observed. Shift in absorption bands of methyl orange after treating with metal nanoparticles strongly indicates the interaction between methyl orange and metal nanoparticles. In spectra of methyl orange treated with metallic nanoparticles, the IR bands observed in range of  $3424$ - $3419 \text{ cm}^{-1}$  can be attributed to N-H stretching of  $\text{NH}_2$ , bands in range of  $1637$ - $1625 \text{ cm}^{-1}$  is of N-H bending, while bands in range of  $1531$ - $1522 \text{ cm}^{-1}$  and  $1354$ - $1321 \text{ cm}^{-1}$  are of asymmetric and symmetric stretching of  $\text{NO}_2$ . From the findings obtained from IR spectra and with reference to

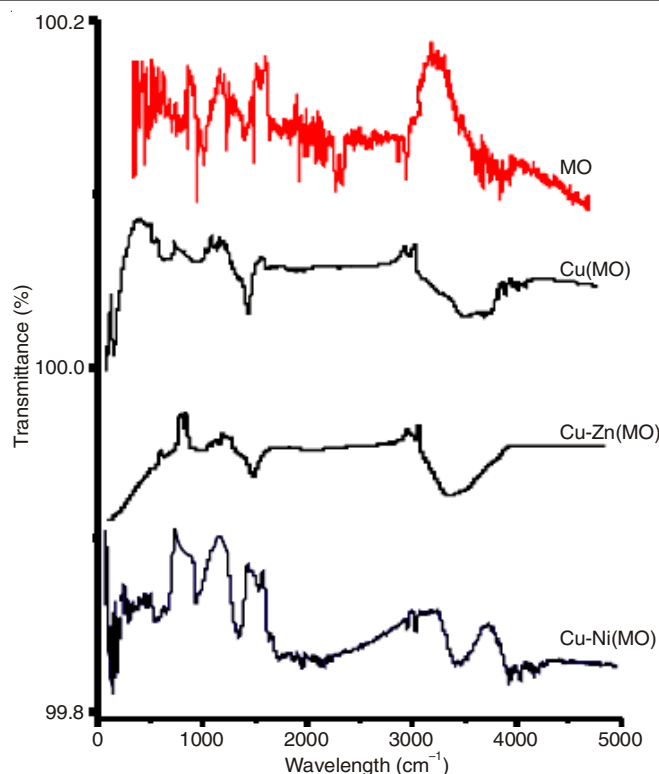


Fig. 7. IR spectra of methyl orange treated with mono and bimetallic nanoparticles

literature [20,21], probable mechanism for the photocatalytic degradation of methyl orange is presented in **Scheme-II**.

To understand the enhancement in the photocatalytic activity of bimetallic particles, the optical band gaps for the different nanocatalyst were calculated using the Tauc relation:

$$\alpha h\nu = B(h\nu - E_g)^n$$

where  $\alpha$  is the absorption coefficient,  $B$  is a constant,  $h\nu$  is the energy of the photons and exponent  $n$  depends on the type of the transition and  $n$  may have values  $1/2$ ,  $2$ ,  $3/2$  or  $3$  corresponding to allowed direct, allowed indirect, forbidden direct or forbidden indirect transitions, respectively.  $\alpha$  and transmittance ( $T$ ) are correlated as

$$T = \exp(-\alpha L)$$

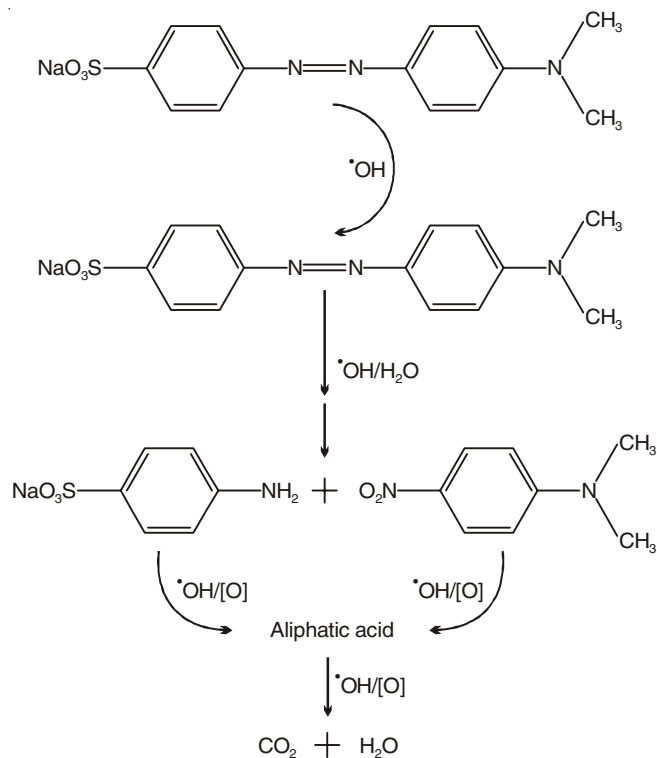
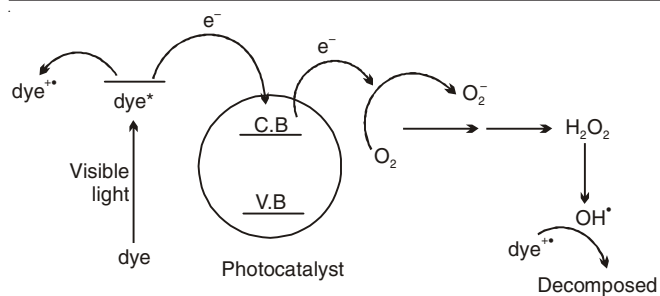
$$\alpha = -(\ln T)/L$$

where,  $L$  is thickness of the sample.

For allowed direct transition  $n = 1/2$  so,

$$(h\nu \ln T)^2 = B^2 L^2 (h\nu - E_g)$$

The exact value of the optical band gap can be obtained by extrapolating the straight-line portion of  $(h\nu \ln T)^2$  vs.  $h\nu$  graph to the  $h\nu$  axis. The band gap so calculated (Fig. 8) are  $2.4 \text{ eV}$  for Cu nanoparticles,  $1.7 \text{ eV}$  for Cu-Ni nanoparticles and  $1.2 \text{ eV}$  for Cu-Zn nanoparticles. Addition of second metal result in narrowing of band gap and such findings are also report earlier in literature [22,23]. With this result it can concluded that with the introduction of second metal to copper nanoparticles, there is significant change in the electronic structure of metal nanoparticles. This narrowing of band gap with addition of second metal allow the electrons in valence band to jump at the conduction band and these electrons in turn generate



**Scheme-II:** Probable mechanism for the photocatalytic degradation of methyl orange by mono and bimetallic nanoparticles

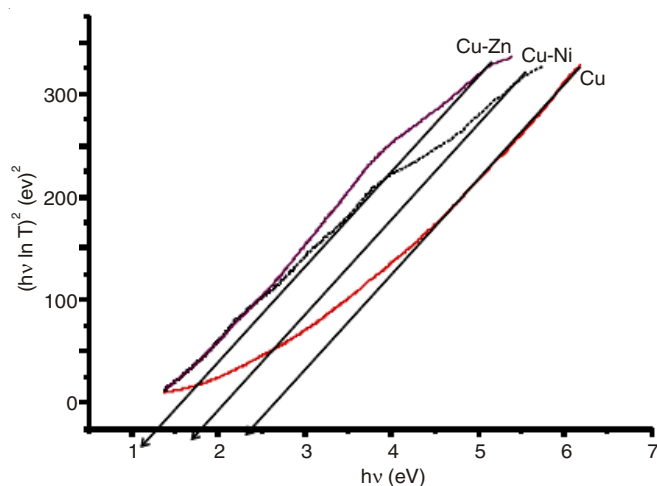


Fig. 8. Plot of  $h\nu$  (eV) against  $(h\nu \ln T)^2$  (eV)<sup>2</sup>

OH radicals (**Scheme-II**) which is responsible for degradation of methyl orange [24-26].

## Conclusion

Monometallic Cu, bimetallic Cu-Ni and Cu-Zn nanoparticles have been synthesized successfully using ascorbic acid as green reducing and capping agent. Route employed for the fabrication is more economy, safe and free from harsh solvents. Bimetallic nanoparticles as prepared are of alloy nature and possess good photocatalytic activity. Degradation reaction of methyl orange followed first order kinetic with rate constant in order of  $k_{\text{Cu-Zn}} > k_{\text{Cu-Ni}} > k_{\text{Cu}}$ . Enhancement of photocatalytic property of bimetallic nanoparticles over monometallic nanoparticles is attributed to the bi-functional effect.

## ACKNOWLEDGEMENTS

The authors are thankful to Physics Department, Manipur University, for recording SEM images and XRD data.

## REFERENCES

1. D.S. Wang and Y. Li, *Adv. Mater.*, **23**, 1044 (2011).
2. B. Xia, F. He and L. Li, *Langmuir*, **29**, 4901 (2013).
3. E. Cottancin, J. Lerme, M. Gaudry, M. Pellarin, J.L. Vialle, M. Broyer, B. Prével, M. Treilleux and P. Mélinon, *Phys. Rev. B*, **62**, 5179 (2000).
4. Y. Mizukoshi, T. Fujimoto, Y. Nagata, R. Oshima and Y. Maeda, *J. Phys. Chem. B*, **104**, 6028 (2000).
5. I.N. Iftikhar and P. Abida, *Turk. J. Chem.*, **29**, 627 (2005).
6. Z. Komeily-Nia, M. Montazer and M. Latifi, *Colloids Surf. A*, **439**, 167 (2013).
7. A. Umer, S. Naveed, N. Ramzan and M.S. Rafique, *NANO Brief Reports and Reviews*, **7**, 1230005 (2012).
8. M.L. Wu, D.L. Chen and T.C. Huang, *Chem. Mater.*, **13**, 599 (2001).
9. N. Toshima and T. Yonezawa, *New J. Chem.*, **22**, 1179 (1998).
10. D. Lahiri, B. Bunker, B. Mishra, Z. Zhang, D. Meisel, C.M. Doudna, M.F. Bertino, F.D. Blum, A.T. Tokuhira, S. Chattopadhyay, T. Shibata and J. Terry, *J. Appl. Phys.*, **97**, 094304 (2005).
11. H.P. Singh, N. Gupta, S.K. Sharma and R.K. Sharma, *Colloids Surf. A*, **416**, 43 (2013).
12. C.C. Wu and D.H. Chen, *Gold Bull.*, **43**, 234 (2010).
13. T.M.D. Dang, T.T.T. Le, E. Fribourg-Blanc and M.C. Dang, *Adv. Nat. Sci. Nanosci. Nanotechnol.*, **2**, 015009 (2011).
14. M.A. Newton and W. van Beek, *Chem. Soc. Rev.*, **39**, 4845 (2010).
15. A.K. Singh and Q. Xu, *ChemCatChem.*, **5**, 652 (2013).
16. H.L. Jiang and Q. Xu, *J. Mater. Chem.*, **21**, 13705 (2011).
17. X. Ji, K.T. Lee, R. Holden, L. Zhang, J. Zhang, G.A. Botton, M. Couillard and L.F. Nazar, *Nat. Chem.*, **2**, 286 (2010).
18. T. Franlin, *Chem. Soc. Rev.*, **41**, 7977 (2012).
19. D.L. Pavia, G.M. Lampman, G.S. Kriz and J.R. Vyvyan, *Introduction to Spectroscopy*, Western Washington University, Bellingham, Washington, Chap. 2, pp. 43-80 (2015).
20. T. Chen, Y. Zheng, J. Lin and G. Chen, *J. Am. Soc. Mass Spectrom.*, **19**, 997 (2008).
21. K. Dai, H. Chen, T.Y. Peng, D. Ke and H. Yi, *Chemosphere*, **69**, 1361 (2007).
22. C.-C. Wang, J.-R. Li, X.-L. Lv, Y.-Q. Zhang and G. Guo, *Energy Environ. Sci.*, **7**, 2831 (2014).
23. A.S. Ahmed, M. Shafeeq M, M.L. Singla, S. Tabassum, A.H. Naqvi and A. Azam, *J. Lumin.*, **131**, 1 (2011).
24. R.B. Sankara, R.S. Venkatramana, R.N. Koteeswara and K.J. Pramoda, *Res. J. Mater. Sci.*, **1**, 11 (2013).
25. M.A. Rauf, M.A. Meetani and S. Hisaindee, *Desalination*, **276**, 13 (2011).
26. I.K. Konstantinou and T.A. Albanis, *Appl. Catal. B*, **49**, 1 (2004).